Global Ecology & Biogeography (2002) **11**, 115–129

RESEARCH ARTICLE

Net primary productivity mapped for Canada at 1-km resolution

J. LIU, J. M. CHEN,* J. CIHLAR and W. CHEN

Canada Centre for Remote Sensing, 588 Booth Street, Ottawa, Ontario K1A 0Y7, Canada. E-mail: chenj@geog.utoronto.ca

ABSTRACT

Aim To map net primary productivity (NPP) over the Canadian landmass at 1-km resolution.

Location Canada.

Methods A simulation model, the Boreal Ecosystem Productivity Simulator (BEPS), has been developed. The model uses a sunlit and shaded leaf separation strategy and a daily integration scheme in order to implement an instantaneous leaf-level photosynthesis model over large areas. Two key driving variables, leaf area index (every 10 days) and land cover type (annual), are derived from satellite measurements of the Advanced Very High Resolution Radiometer (AVHRR). Other spatially explicit input data are also prepared, including daily meteorological data (radiation, precipitation, temperature, and humidity), available soil water holding capacity (AWC) and forest biomass. The model outputs are compared with ground plot data to ensure that no significant systematic biases are created.

Results The simulation results show that Canada's annual net primary production was 1.22 Gt C year^{-1} in 1994, 78% attributed to forests, mainly the boreal forest, without considering the contribution of the understorey. The NPP averaged over the entire landmass was ~140 g C m^{-2} year^{-1} in 1994. Geographically, NPP varied greatly among ecozones and provinces/territories. The seasonality of NPP is characterized by strong summer photosynthesis capacities and a short growing season in northern ecosystems.

Conclusions This study is the first attempt to simulate Canada-wide NPP with a process-based model at 1-km resolution and using a daily step. The statistics of NPP are therefore expected to be more accurate than previous analyses at coarser spatial or temporal resolutions. The use of remote sensing data makes such simulations possible. BEPS is capable of integrating the effects of climate, vegetation, and soil on plant growth at a regional scale. BEPS and its parameterization scheme and products can be a basis for future studies of the carbon cycle in mid-high latitude ecosystems.

Key words Biogeochemical processes, boreal forest, Canada, ecological modelling, net primary productivity, remote sensing, terrestrial carbon.

INTRODUCTION

Net primary productivity (NPP) is a quantitative measure of the carbon absorption by plants per unit time and space. NPP data are useful in many applications, such as terrestrial carbon cycle research (Bonan, 1995; Hunt *et al.*, 1996; Chen J *et al.*, 2000; Chen W *et al.*, 2000) and studies of regrowth following forest fires (Amiro *et al.*, 2000). Due to their time- and labour-intensive nature, ground measurements of NPP are very limited in temporal and spatial coverage. It is therefore necessary to use computer models, calibrated with existing data, in combination with remote sensing and other datasets, to study the spatial and temporal variations of NPP.

Process models for estimating NPP simulate a series of plant physiological processes, including photosynthesis, autotrophic respiration and transpiration. Process models have the advantages of: (1) being theoretically grounded, (2) the ability to handle interactions and feedbacks of different processes, (3) the flexibility to describe details of biological processes under a variety of conditions, and (4) the verifiability of explicit hypotheses regarding plant physiological processes. However, the application of models of this type is hindered by data availability and computing resources. Another challenge is the need for temporal and spatial scaling of a process model, because most process models have been

* Corresponding author: J. M. Chen, Department of Geography, University of Toronto, 100 St George Street, Toronto, Ontario, Canada M5S 3G3. E-mail: chenj@geog.utoronto.ca

Table 1 Major vegetation parameters for different Canadian land cover types

Parameter	Coniferous forest	Mixed forest	Deciduous forest	Crop	Grass	Reference
Maximum stomatal conductance (mm s^{-1})	1.0	3.0	5.0	5.0	5.0	Running & Hunt (1993); Kimball *et al.* (1997)
Clumping index	0.5	0.6	0.7	0.9	0.9	Liu *et al.* (1997)
Maximum carboxylation at 25 °C (μmol CO_2 m^{-2} s^{-1})	33	33	33	50	33	Bonan (1995)
Specific leaf area* (m^2 kg C^{-1})	10	25	40			Middleton *et al.* (1997)

* Specific leaf area is not provided for nonforest land covers because the parameter is not required for these land cover types in the model.

originated at leaf or stand levels (Chen *et al.*, 1999). Modellers often have to juggle between spatial resolutions and model execution time steps. To our knowledge, the finest spatial resolution a process model of global coverage or subcontinental (e.g. USA) coverage has achieved is 0.5° × 0.5° (Melillo *et al.*, 1995; Cramer *et al.*, 1999).

Remotely sensed data are important in providing spatially explicit inputs for process models. These include vegetation indices as the key driving variables (Running *et al.*, 1989; Hunt *et al.*, 1996; Sellers *et al.*, 1996; Liu *et al.*, 1997) and land cover types in recognition of substantial physiological differences among vegetation types (Bonan, 1993; Liu *et al.*, 1997).

In this paper, we shall describe a process-based model for estimating NPP across Canada at a moderate resolution (~1 km), using nationwide input datasets derived from satellite images and from other sources.

DESCRIPTION AND EXECUTION OF THE MODEL

The process model, dubbed the Boreal Ecosystem Productivity Simulator (BEPS), was originally built using biological principles in forest biogeochemical cycles (FOREST-BGC) (Running & Coughlan, 1988) with some modifications (Liu *et al.*, 1997). The model has been refined by incorporating an advanced photosynthesis model, the Farquhar model (Farquhar *et al.*, 1980). The instantaneous model at the leaf level was scaled to the whole canopy for a day, using a temporal and spatial integration scheme (Chen *et al.*, 1999). This improved version of BEPS (Chen *et al.*, 1999; Liu *et al.*, 1999) was used for estimating NPP across Canada. Detailed descriptions of model structure, simulation of photosynthesis, plant respiration and other biological processes are available in Liu *et al.* (1999). Key model equations are described in Appendix 1 and major vegetation parameters are listed in Table 1. As a process-based ecosystem model, BEPS is sensitive to environmental conditions and plant characteristics. Intensive sensitivity analysis to environmental conditions and plant characteristics was carried out in another study, along with eight other ecosystem models (Potter *et al.*, 2001).

To execute BEPS over Canada's landmass, spatially explicit input data were prepared. Land cover and leaf area index maps were derived from satellite images, while soil and meteorological data were obtained from other sources (Liu *et al.*, 1999). The land cover and leaf area index maps are at 1-km resolution in a Lambert conformal conic (LCC) projection (49° and 77°N standard parallels, 95°W meridian). Other data with different formats were reprocessed into the same resolution (1 km) and projection (LCC) as the satellite data, either prior to or during the model execution. The temporal intervals of the input data are: annual for land cover; 10 days for leaf area index during the growing season; daily for meteorological data; and long-term for soil.

The year 1994 was selected for our first attempt to assess the NPP distribution over Canada because: (1) algorithms for deriving LAI were developed using extensive ground measurements made in that year, (2) several intensive 1994 field campaigns of the BOREAL Ecosystem-Atmospheric Study (BOREAS) (Sellers *et al.*, 1995) produced data that are useful for both model and map validations, and (3) it was a relatively normal year according to the 100-year trend of annual mean air temperature for Canada (Fig. 1) (Environment Canada, 2000).

BEPS simulated NPP in 1994 pixel by pixel at a daily step through the whole year. The domain covers Canada with 5700 pixels by 4800 lines at 1-km resolution. On the first day, snow pack data were entered into the model. Snow and rain were differentiated by air temperature in the model.

It should be pointed out that, in this study, forest NPP only represents the NPP of the overstorey (i.e. trees including leaf, stem and root). The understorey's contribution is excluded since the LAI data only include the overstorey LAI. This is not an issue for other non-forest land cover types.

MODEL INPUT DATA

Land cover

Ecosystem type and characteristics are among the basic variables determining the magnitude of the various terrestrial carbon

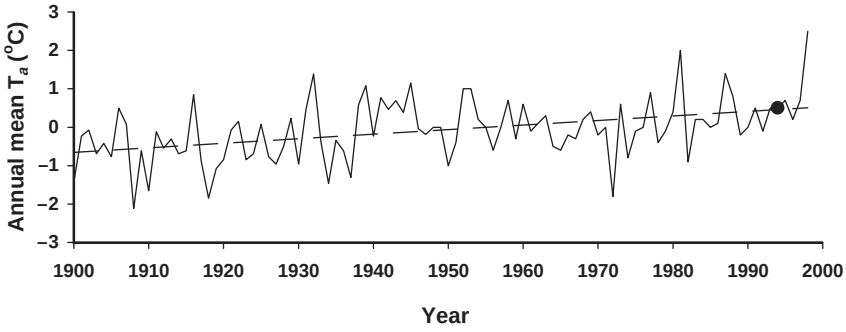

Fig. 1 Canada's mean daily air temperature over 100 years. The dashed line denotes the long-term trend. The dot indicates 1994.

pools as well as the fluxes among them. The effect of various ecosystem characteristics can be parameterized in biogeochemical models such as BEPS, provided that information on the distribution of land cover types is known. Over large areas, satellite remote sensing is the only viable method for obtaining such up-to-date information. Although there are several global or Canadian land cover products available at a similar resolution (Pokrant, 1991; Olson, 1994; Belward, 1996), efforts have been made here to create a land cover map for Canadian application with enhanced accuracy (Pietroniro & Soulis, 1999).

The land cover map was derived from the Advanced Very High Resolution Radiometer (AVHRR) data on board the NOAA-14 satellite and obtained during 1995. In order to remove or minimize errors due to sources unrelated to the land surface characteristics in the raw satellite signals, a series of correction procedures were used, including sensor calibration, geometrical registration and image composition over 10-day periods. The composite images were further corrected for atmospheric aerosol and water vapour effects, bidirectional reflectance variations, residual clouds and subpixel contamination and temporal trajectories by smoothing (Cihlar, 1996; Cihlar *et al.*, 1997a, 1997b).

Given the large area of Canada and the lack of knowledge regarding the spectral and temporal behaviour of the diverse terrestrial ecosystems, our approaches are based on unsupervised classification strategies that assume no prior knowledge of the thematic content of the satellite data. The objective is to extract all land cover information contained in the corrected satellite data, to enable the assignation of spectrally pure clusters to individual land cover classes. A land cover map (Cihlar *et al.*, 1999) was prepared from the processed AVHRR data using the Enhancement-Classification Method (ECM; Beaubien *et al.*, 1999). The classification employed surface reflectance values of AVHRR channel 1, channel 2 and the Normalized Difference Vegetation Index (NDVI). For each channel, the data were averaged over the growing season, after determining its length on a pixel basis using surface temperature estimated from AVHRR channels 4 and 5 after corrections for surface emissivity (Cihlar *et al.*, 1997b).

By collapsing the 31 cover types thus obtained into 10 groups, we obtained an overview of land cover of Canada at 1-km resolution (Table 2). 42% of the Canadian landmass was found to be covered mainly by needleleaf coniferous and mixed forest, with a smaller presence of broadleaf deciduous forest. Other large land components were barren land and shrubland in the north, which account for 28% and 11% of the total land area, respectively. The remaining cover types occupied relatively small portions of the total area.

Forested areas spread from the southern border to 66°N with the highest density around 50–54°N. Cropland and grassland were mainly located south of 54°N, while shrubland spread over areas north of 46°N. Dominant cover types in the north were barren land and snow or ice areas, diminishing gradually southward. Urban areas were scattered mostly below 54°N, while burnt areas appeared more in the north.

Table 2 Land cover statistics of Canada at 1-km resolution

Land cover type	Total pixels*	Land cover/ total land (%)
Coniferous forest	2 642 329	29.6
Mixed forest	1 121 650	12.6
Deciduous forest	40 240	0.5
Shrubland	986 365	11.1
Burnt area	225 228	2.5
Barren land	2 496 086	27.9
Cropland	670 235	7.5
Grassland	51 615	0.6
Urban area	9 211	0.1
Snow/ice	690 477	7.7
Total land	8 933 436	100.0
Total forest	3 804 219	42.6

* 1 pixel ≈ 1 km^2.

Leaf area index (LAI)

The same correction procedures for land cover mapping were employed for generating LAI maps from raw AVHRR data in 1994. In previous studies, ground measurements were made and correlated with Landsat TM images (Chen & Cihlar, 1996). TM LAI images at 30-m resolution were scaled to AVHRR imagery at 1-km resolution after coregistering the two images at the same time. The simple ratio (SR), the ratio of the reflectance of near infrared to the reflectance of red, was chosen to derive LAI because of its greater resolution of high LAI values than the normalized difference vegetation index (NDVI). It was found that TM SR is 28% higher than AVHRR SR, mainly due to the difference in bandwidths of the two sensors. After correcting for this, the formulae relating LAI to SR for AVHRR imagery were developed for the various land cover types based on our previous studies and the literature (Asrar *et al.*, 1984; Aase *et al.*, 1986; Wiegand *et al.*, 1992; Li *et al.*, 1993; Chen & Cihlar, 1996). The formulae for the various land cover types are given in Chen *et al.* (2002).

In a normal year, 10-day 'cloud-free' composite AVHRR images are used to generate 20 LAI images from April 11 to October 31, a span covering most of the growing season in Canada. The 'cloud-free' composites were produced for cloudy regions through a residual cloud elimination scheme using albedo and NDVI trends (Cihlar, 1996). Because of the NOAA 11 AVHRR sensor failure in early September 1994, only the first 15 satellite images became available. The rest of the five images were supplemented with the LAI images over the same period in 1993. This treatment will bring some uncertainty to the NPP estimation. However, as discussed below, < 3% of annual modelled NPP was produced in that period. It is assumed that there was not much change in LAI beyond the growing season and consequently LAI before April 11 and after October 31 was set to be the same as that on April 11 and October 31, respectively.

Table 3 shows mean LAI values of the 20 images for different vegetation types in 1994. The mean LAI was generally high for forest. Cropland and grassland had mean LAI values of 1.2 and 0.5, respectively. Mean LAI values for urban, shrub, burnt, and barren land cover types were less than 1.0. These LAI values are close to those simulated by the CARbon Assimilation In the Biosphere model (CARAIB) (Warnant *et al.*, 1994), and variously lower or higher than those from other models (Bondeau *et al.*, 1999). Validation of Canada-wide LAI maps using ground data collected within eight Landsat scenes distributed across Canada has been performed (Chen *et al.*, 2002).

Soil data

Available soil water-holding capacity (AWC) is defined here as the portion of water in the soil that can readily be extracted by plant roots. It is usually considered as the water held in the root zone between field capacity and wilting point, a pressure of up to approximately 15 bars (Shields *et al.*, 1991). AWC is the single soil variable required by BEPS for this study. The AWC data were obtained from the Soil Landscapes of Canada (SLC) database, the best soil database currently available for the country (Shields *et al.*, 1991). AWC is available in SLC version 1.0 only, with missing values in some areas of the country. To fill the gaps, the dominant soil texture of a polygon in SLC version 2.0 was processed. AWC was then derived from its relationship with soil texture (De Jong *et al.*, 1994). To generate an AWC layer with the same projection and resolution as the other data layers, the original vector data in SLC were mosaiced, reprojected, and rasterized in a geographical information system (ARC/INFO).

When snow exists on the ground soil water is defined, in the model, to be unavailable to plants. Therefore photosynthesis is very small in early spring even when the radiation is abundant and air temperature is above freezing point (Frolking, 1997). Snow pack thickness varies with air temperature, radiation, and previous and new snow, as snow melt and sublimation are calculated as a function of air temperature and radiation. This simple treatment is effective in dealing with the problem of low soil temperature in permafrost and semipermafrost areas.

Statistics show that AWC is generally higher in cropland and pasture than in forest and shrubland (Table 3). Deciduous and mixed forests have slightly higher AWC than coniferous forests.

Table 3 LAI and AWC by vegetation type

Vegetation type	LAI		AWC (m)	
	Mean	SD	Mean	SD
Coniferous forest	2.7	1.4	0.11	0.04
Mixed forest	2.9	1.0	0.12	0.06
Deciduous forest	3.0	0.8	0.12	0.04
Shrubland	0.8	0.5	0.12	0.06
Cropland	1.2	0.7	0.17	0.04
Grassland	0.5	0.3	0.16	0.06
Forest	2.7	1.2	0.11	0.06
Land	1.4	1.4	0.13	0.08

'Forest' refers to all forest land, 'Land' all land excluding water body; SD: standard deviation.

Meteorological data

Meteorological data were obtained from the median range forecast (MRF) Global Flux Archive from the National Center for Environmental Prediction (NCEP), distributed by the National Center for Atmospheric Research (NCAR). The

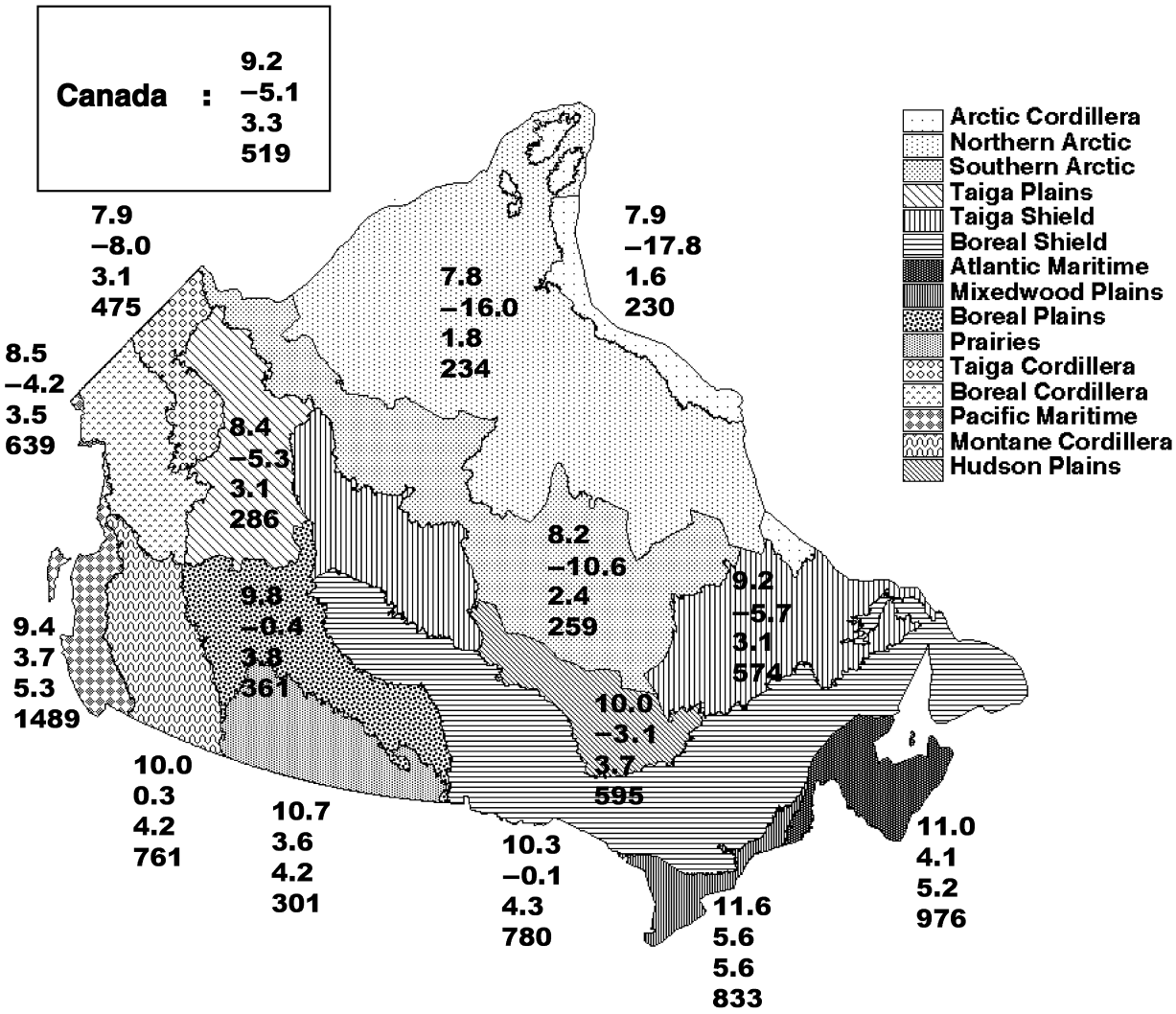

Fig. 2 Annual statistics of meteorological parameters by ecozone for Canada in 1994: daily mean radiation in MJ m^{-2} day^{-1} (row 1), daily mean air temperature in °C (row 2), daily mean specific humidity in g kg^{-1} (row 3), and yearly total precipitation in mm $year^{-1}$ (row 4). The values in a box are the means of the parameters for Canada.

dataset was chosen because it contains variables of interest (radiation, temperature, humidity, precipitation and snow pack) at appropriate temporal intervals (daily) and spatial resolution (a Gaussian grid system at ~0.9° interval, varied with longitude and latitude) over the country. All meteorological parameters are bilinearly interpolated daily for each pixel during the execution of the model.

The daily radiation, temperature and precipitation in the NCAR dataset were compared with the measurements made in 1994 at up to 60 stations over Canada, with over 5000 samples for each parameter. As found in a previous study (Liu *et al.*, 1997), daily total radiation in the NCAR data was generally 30–40% higher than the ground measurements, mainly because of the neglect of radiation absorption by aerosols in the models generating the NCAR dataset. This is corrected in BEPS using a coefficient of 0.62 for 1994. The observed daily mean temperatures agreed relatively well with the NCAR data (r = 0.93). The mean difference between the observed and NCAR precipitation was 0.13 mm/day, with a standard deviation of 5.3 mm, indicating a large scatter of the differences.

Figure 2 shows the annual statistics of radiation, temperature, humidity and precipitation in 1994 for each ecozone (Ecological Stratification Working Group, 1995), based on the interpolated NCAR data. Latitudinal gradients of radiation, temperature, and humidity were evident over Canada's landmass. Precipitation was higher for the west and the east coasts than in the interior.

Forest biomass data

Biomass is a critical parameter determining respiration, but currently there are no mature techniques for mapping biomass distribution for large areas. In regional estimation of NPP, two methods are often used to reduce this data constraint. One is to assign representative biomass values by cover type (Foley, 1994; Melillo *et al.*, 1995; Liu *et al.*, 1999). The other method is to relate the total biomass to remotely sensed LAI or vegetation indices (Bonan, 1995; Hunt *et al.*, 1996). Linear relationships between biomass and LAI were used in these studies. The first method is simple, but errors for individual pixels can sometimes be considerable because the estimated NPP can be negative for stands with low LAI where the assigned biomass values become disproportionally high. The second method can be accurate for nonforest cover types, but problematic for forest types where the total biomass is not only related to LAI but also to the duration of biomass accumulation, i.e. stand age.

In this study, spatially explicit forest biomass data at 1-km resolution were resolved from existing data. Siltanen & Price (2001) derived a dataset of above-ground biomass of forest at 10-km resolution from Canada's Forest Inventory (Lowe *et al.*, 1996; Penner *et al.*, 1997). Using the biomass data and mean LAI averaged from the 20 images, the relationship between the two parameters was first formulated with the two datasets at 10-km resolution. Secondly, above-ground biomass at 1-km resolution was determined by the formulae given below. At the first step, the LAI was resampled to 10-km resolution. The pixels at 10-km resolution were selected where a forest type at 1-km resolution covers more than 90% of the total 100 km^2 area. There were 2758 samples for coniferous forest satisfying the threshold, 448 for mixed forest, and 0 for deciduous forest. Although the data were scattered, general trends could be resolved, especially for coniferous forest. The following formulae were obtained by fitting the data points with quadratic equations of zero interception:

Coniferous forest: $B = 0.9097LAI + 0.125LAI^2$
($r^2 = 0.219$, SE = 0.017, $P > 0.01$, $n = 2758$)
Mixed forest: $B = 1.545LAI + 0.183LAI^2$
($r^2 = 0.095$, SE = 0.045, $P > 0.01$, $n = 448$)

where B is above-ground biomass in kg m^{-2}; SE, standard error. Generally, the biomass of mixed forest increases with LAI faster than that of coniferous forest. Because limited information about deciduous forest was available, the equation for mixed forest was used for the deciduous cover type. This may underestimate the biomass of deciduous forests. It is understandable that large uncertainties still exist even after the best available biomass data are used. However, we contend that the methods used in this study are improvements over existing methods for Canada.

The total root biomass was separated into fine root and coarse root components using a relationship established by Kurz *et al.* (1996). In this way, the fine root biomass does not increase linearly with LAI, but reaches an asymptotic value. This avoids the problem of overestimating root respiration and underestimating NPP at high LAI. Coarse root and fine root biomass were derived from their relationships with above-ground biomass for different forest types (Kurz *et al.*, 1996). While root biomass and stem biomass (~90% of above-ground biomass) were fixed for the year, leaf biomass was calculated daily from the ratio of daily LAI to specific leaf area.

RESULTS AND DISCUSSION

Validation of the NPP map

The NPP map derived from BEPS was tested against field data from six sites in the BOREAS region (Ryan *et al.*, 1997) and 31 sites in Quebec province (Gagnon *et al.*, 1994). Good agreement between the field and modelled overstorey NPP values is found at the BOREAS sites ($r^2 = 0.79$, $P < 0.05$, and SE = 0.23) (Table 4). The mean relative difference between

Table 4 Comparison of the modelled overstorey NPP in 1994 with field data at the BOREAS sites

Site	Longitude (degree)	Latitude (degree)	Field NPP (g C m^{-1} year^{-1})	Modelled NPP (g C m^{-1} year^{-1})	Relative difference (%)
OJP_N	98.62w	55.927n	218	310	42
OBS_N	98.48w	55.879n	243	290	19
OA_N	98.405w	55.532n	386	360	–7
OJP_S	104.69w	53.916n	230	270	17
OBS_S	105.12w	53.895n	298	315	6
OA_S	106.20w	53.629n	374	395	6
Mean			292	323	14

Field data are cited from Ryan *et al.* (1997). 'OJP' denotes old jack pine, 'OBS' old black spruce, 'OA' old aspen. The subscripts 'N' and 'S' denote the northern study area and the southern study area in the BOREAS region, respectively. The comparison statistics are as $r^2 = 0.79$, $P < 0.05$, SE = 0.23.

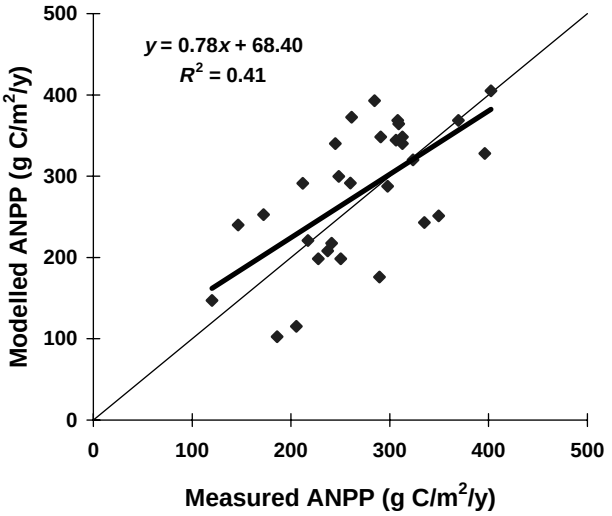

Fig. 3 Comparison of modelled and measured above-ground NPP of the overstorey at some forest sites in the province of Quebec. The ratio of carbon to biomass is taken as 0.5 (Bonan, 1995).

the two datasets is 14%, with a maximum of 42% at the old jack pine site in the northern study area. The root-mean-square error of modelled NPP is 48 g C m^{-2} $year^{-1}$, i.e. 16% of mean NPP in the ground dataset. The above-ground NPP (ANPP) data in Quebec were derived from biomass in the Le réseau de surveillance des écosysèmes forestiers (RESEF) database (Gagnon *et al.*, 1994). It represents long-term averaged overstorey ANPP in the 31 forest sites, each of which is about 50 × 50 m in dimensions. The modelled overstorey ANPP at 1 × 1-km captures and returns a significant, but not high, portion of the variation in the ground data (r^2 = 0.41, P < 0.01, SE = 0.14) (Fig. 3). Note that the year for the comparison was the same for the BOREAS sites, while for the sites in Quebec, the comparison was made between the year 1994 and the long-term averages. Both comparisons suffer from the same scale difference: the ground plots are of the order of tens of metres, while the satellite-based NPP values are the means of 1 × 1-km areas using gridded climate and other input data instead of 'real' site data. The spatial heterogeneity within grid cells must have contributed considerably to the differences in comparisons. The comparisons nevertheless allow us to examine any biases in the modelled NPP values and thus give confidence in the model performance.

NPP distribution over Canada

The BEPS-simulated annual NPP distribution in Canada in 1994 is shown in Fig. 4. High NPP values were associated with forested areas across the country from west to east. The highest NPP, > 700 g C m^{-2} $year^{-1}$, appeared in the south-east part of Vancouver Island, Lower Mainland and coastal Pacific Ranges. Areas with NPP values around 500 g C m^{-2} $year^{-1}$ were located within interior British Columbia, central Alberta, and southern Ontario and Quebec. In the far north, with mainly snow, ice, bare soil and rock, NPP was < 1 g C m^{-2} $year^{-1}$. Comparing these results with 11 models applied at the global scale, mainly with 1931–60 long-term climate data (Bondeau *et al.*, 1999), our NPP values over the region east of 90°W are close to the results from the CASA (Potter *et al.*, 1993), and BIOME3 models (Haxeltine & Prentice, 1996), which are in the low range among the 11 models. The range of our NPP values for Canada is similar to that estimated using a dynamic vegetation model (Woodward *et al.*, 1995). The NPP range for boreal forest is also comparable with a previous study (Peng & Apps, 1999).

NPP by land cover

The simulated NPP values depended greatly on vegetation type and density (Fig. 5a). In national averages, deciduous and mixed forests had the highest capability of absorbing carbon per unit surface area, followed by crop, coniferous forest and grass. Mean NPP values in shrubland, burnt area, barren land and urban area were much smaller. In consequence, the average annual overstorey NPP for forested areas was 251 g C m^{-2} $year^{-1}$ while the national mean NPP was 136 g C m^{-2} $year^{-1}$. Although coniferous forests were only about half as productive as deciduous forests per unit area, the coniferous forests, as a whole, contributed the greatest portion, i.e. 44.2%, to the country's annual NPP because of their large coverage (Fig. 5b). Mixed forest and crop made 32.7% and 12.4% contributions, respectively. Total national annual NPP was estimated to be 1.22 Gt in 1994.

The above discussion excludes understorey NPP for forest cover types. According to Ryan *et al.* (1997), understorey NPP accounted for 8–18% of the overstorey NPP in two aspen stands, and 3–5% in some spruce and pine stands at the BOREAS sites in 1994. Taking 4%, 8% and 13% of overstorey NPP to represent understorey NPP for coniferous, mixed and deciduous forest, national mean NPP values for coniferous, mixed, and deciduous forests, including both understorey and overstorey, were 210, 385, 440 g C m^{-2} $year^{-1}$, respectively. On this basis, the average annual NPP for forest areas was 264 g C m^{-2} $year^{-1}$ while the national mean NPP was 143 g C m^{-2} $year^{-1}$. As a result, total national annual NPP was 1.27 Gt C in 1994. This is 2–3% of estimated global annual NPP, which itself ranges from 39.9 to 80.5 Gt C $year^{-1}$ among various models (Cramer *et al.*, 1999).

To assess NPP values for cropland, data for yield and cultivated area of all crops were collected from Statistics Canada (1995). After converting the yield into NPP with consideration of water content and biomass factors, the mean NPP of crops in Canada was estimated to be ~280 g C m^{-2} $year^{-1}$ in the year, higher than the value of ~220 g C m^{-2} $year^{-1}$ found

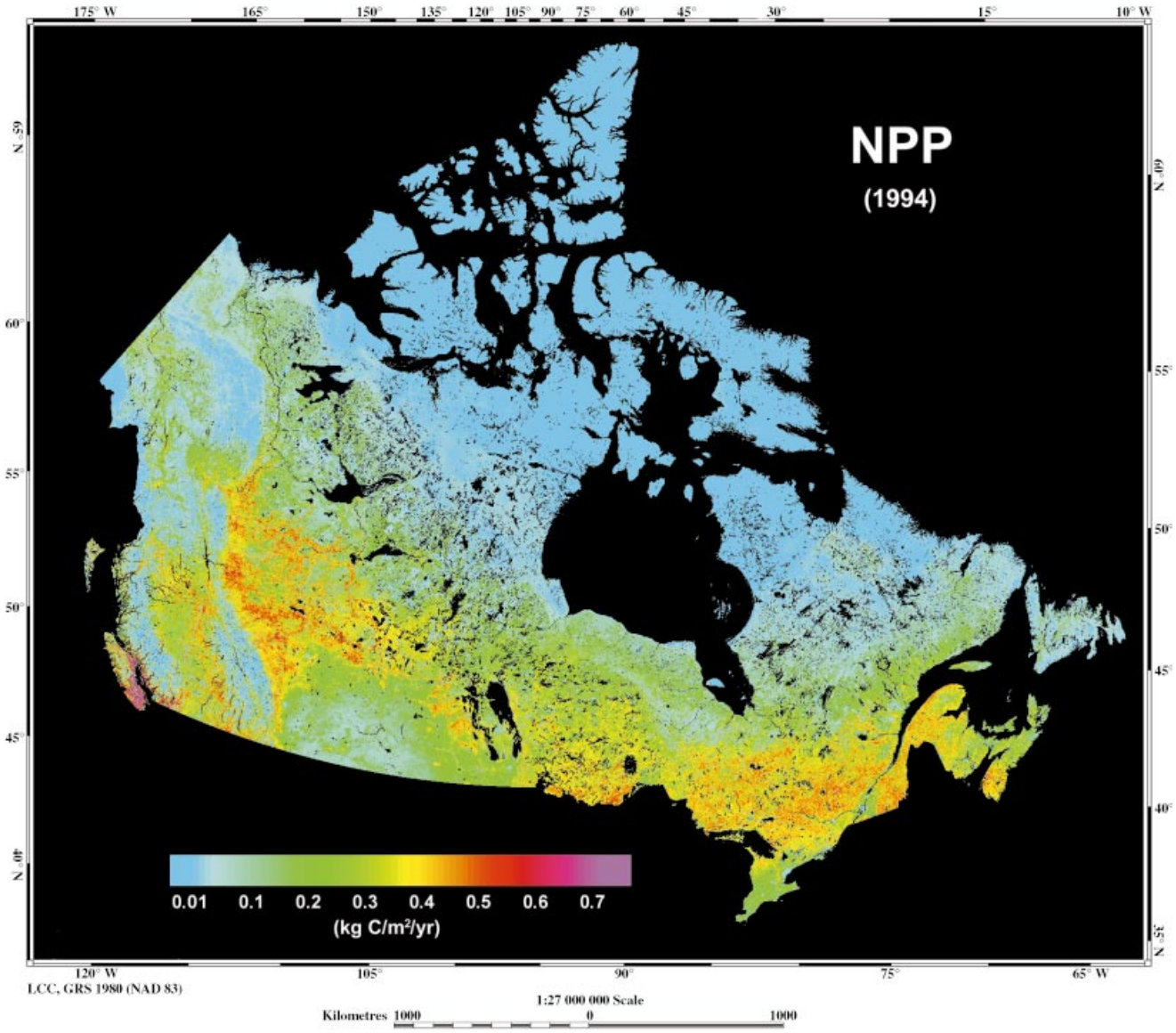

Fig. 4 BEPS-simulated NPP map of Canada in 1994.

in this study. This difference may be due to the fact that pixels labelled as cropland in the satellite land cover map at 1-km resolution often include both crops and other nonproductive cover types, such as roads and water bodies.

NPP by ecozone and by province and territory

The NPP is summarized by ecozone in Table 5. Boreal Plain, Atlantic Maritime and Mixedwood Plains had mean NPP > 250 g C m^{-2} $year^{-1}$ due to their large portions of forested areas or southern locations or both. Ecozones with mean NPP ranging from 150 to 250 g C m^{-2} $year^{-1}$ included Boreal Shield, Montane Cordillera, Pacific Maritime, Prairies, and Taiga Plains. Further north, in Hudson Plain and Boreal Cordillera, mean NPP values were about 130 g C m^{-2} $year^{-1}$. In the Arctic and the other taiga ecozones, the mean NPP values were < 60 g C m^{-2} $year^{-1}$. For the total primary production in an ecozone, Boreal Shield was larger by far than other ecozones, having a total NPP of 409 Mt C $year^{-1}$. The next largest was Boreal Plains. The rest of the ecozones had total productions between 30 and 100 Mt C $year^{-1}$, except for the four Arctic and taiga ecozones, for which the total production was very low.

The NPP varied greatly by province/territory due to large differences in land area and diversity in land cover (Table 6).

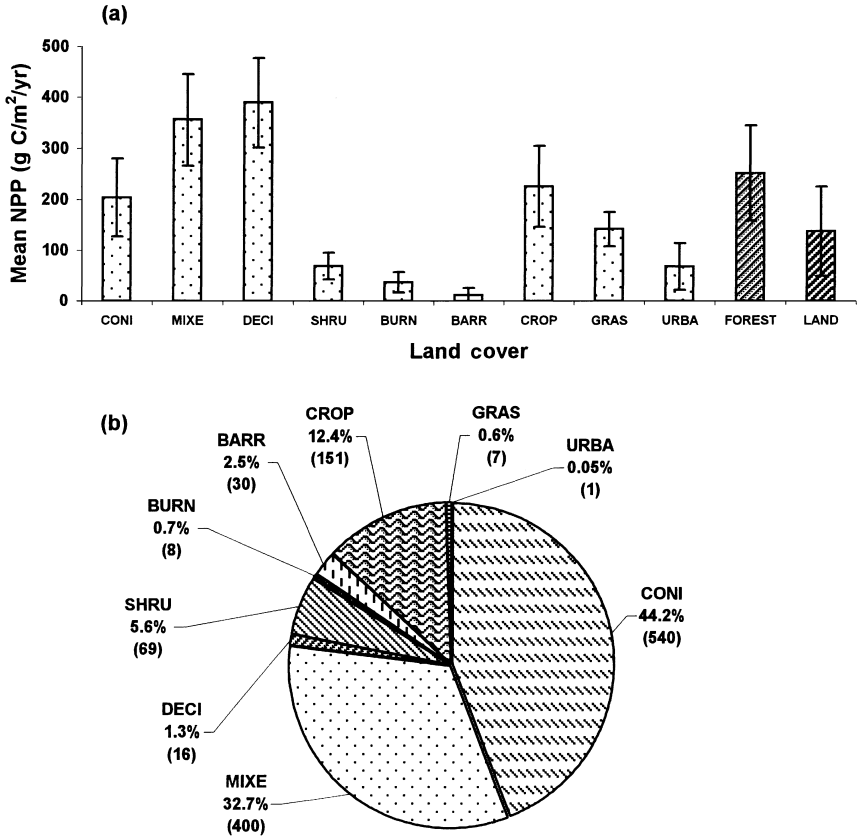

Fig. 5 NPP by land cover in 1994 (a) class mean NPP and (b) class total NPP. Note the last two bars are summary groups. The vertical bars indicate the standard deviation. Values in brackets in Fig. 5b are class total NPP in Mt C year^{-1}. Coni = coniferous forest, Mix = mixed forest, Deci = deciduous forest, Shru = shrubland, Burn = burnt areas, Barr = barren land, Crop = cropland, Gras = grassland, Urba = urban areas.

In provinces/territories dominated by forest, mean NPP was usually high. High values of total production occurred in Ontario, Quebec, British Columbia and Alberta, while the low values were associated with provinces or territories with either small area or low mean NPP.

Seasonal variation

Because of Canada's northern location, short growing seasons and high summer NPP are apparent (Fig. 6). The mean growing season started in April and ended in October (Fig. 6a). NPP of cropland peaked in July, 1994, while NPP of forests in July was slightly lower than that in June. Monthly NPP averaged over Canada followed similar patterns to those of forests, but with a lower value than those of forests and cropland. In the BOREAS experiment, CO_2 fluxes into an aspen stand were observed between the middle of May and the end of September, reaching maximum around the end of June (Black *et al.*, 1996). The flux into a mature black spruce peaked around the beginning of July (Goulden *et al.*, 1997). Seasonal curves of simulated NPP varied among ecozones due to different compositions of land cover and geographical locations (Fig. 6b). The curves in the selected ecozones present various patterns: (1) the peak occurred in July for Pacific Maritime, (2) the peak lasted for 2 months in June and July for Hudson Plains and Boreal Plains, and (3) the peak lasted for 3 months from June to August for Mixedwood Plains.

Characteristics of modelled results

In order to evaluate and appreciate the NPP statistics given above, we provide the following summary of characteristics of our modelling methodology.

1 The regional and temporal statistics are obtained through calculations at daily steps at 1-km resolution. It is the first time that such computations have been made for all Canada or for any other comparable region. The statistics are therefore potentially more accurate than previous results obtained for Canada at coarser spatial or temporal resolutions. The use of remotely sensed land cover and LAI maps made such calculations possible.

Table 5 NPP by ecozone for Canada

Ecozone	Class Mean NPP (SD) (g C m^{-2} $year^{-1}$)	Class Total pixels* (thousand)	Class Total NPP (Mt C $year^{-1}$)
Arctic Cordillera	0 (2)	241	0
Northern Arctic	0 (2)	1421	0
Southern Arctic	15 (24)	741	11
Taiga Cordillera	44 (50)	251	11
Taiga Shield	57 (61)	1148	65
Boreal Cordillera	130 (104)	436	57
Hudson Plains	138 (84)	354	49
Taiga Plains	171 (126)	548	93
Prairies	179 (85)	452	81
Pacific Maritime	189 (194)	197	37
Montane Cordillera	215 (138)	466	100
Boreal Shield	240 (130)	1705	409
Mixedwood Plains	257 (110)	115	30
Atlantic Maritime	310 (110)	201	62
Boreal Plains	321 (124)	656	211
Canada land	136 (145)	8933	1215

* 1 pixel ≈ 1 km^2. The bracket denotes the standard deviation.

Table 6 NPP by province and territory for Canada

Province/ territory	Class Mean NPP (SD) (g C m^{-2} $year^{-1}$)	Class Total pixels* (thousand)	Class Total NPP (Mt C $year^{-1}$)
British Columbia	210 (79)	887	186
Alberta	282 (70)	625	176
Saskatchewan	205 (58)	581	119
Manitoba	197 (59)	537	106
Ontario	259 (59)	926	240
Quebec	143 (73)	1353	193
New Brunswick	302 (49)	71	22
Prince Edward Island	193 (32)	5	1
Nova Scotia	278 (55)	53	15
Newfoundland	43 (23)	354	15
Yukon Territory	102 (46)	450	46
North-west Territories	78 (44)	1130	88
Nunavut Territory	4 (5)	1879	7
Canada land	136 (73)	8933	1215

* 1 pixel ≈ 1 km^2. The bracket denotes the standard deviation.

2 The computations are based on simulations of simplified biological and physical processes rather than empirical methods. BEPS uses a sunlit and shaded leaf separation strategy and a daily integration scheme in order to implement an instantaneous leaf-level photosynthesis model, the Farquhar model, on remotely sensed data. It is therefore capable of integrating the effects of climate, vegetation type and density, soil texture, etc. on plant growth and NPP. It avoids problems of empirical models for which substantial empirical data are required for regional applications. This spatially and temporally upscaled Farquhar model incorporates the nonlinear effects of meteorological

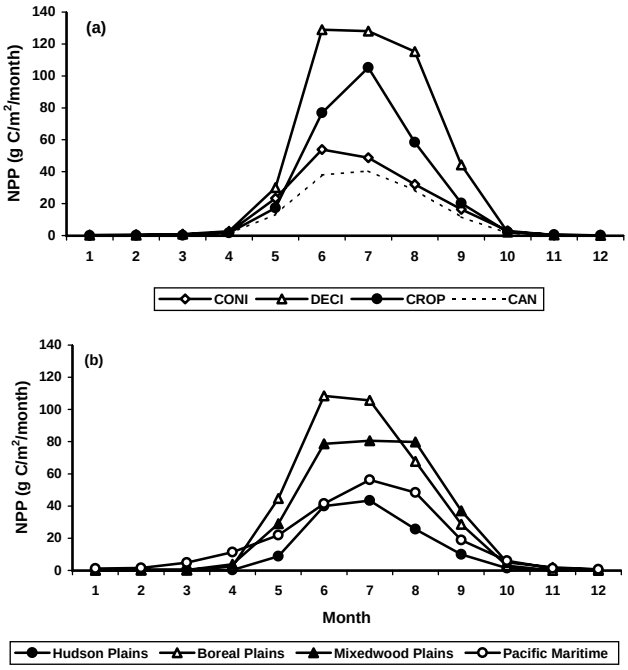

Fig. 6 Monthly NPP (a) by land cover type and (b) by ecozone.

variation within the day and the stand. Because of this process-based modelling methodology, we believe that our NPP statistics provide reasonable estimates for areas without empirical data.

3 An important aspect of BEPS is the consideration of the foliage clumping effect. The clumping reduces sunlit leaves and increases shaded leaves, and the NPP values calculated using the sunlit/shaded leaf scheme are therefore sensitive to canopy architecture. Because of this, the NPP values are smaller than some previous studies that assumed random distributions of leaves and caused different degrees of overestimation of absorbed radiation for different cover types.

4 The components of BEPS have been validated using detailed stand level data to ensure the sensitivity of the model to input variables, and the final model outputs have been compared to ground plot data to ensure that no significant systematic biases are created. These tests of model sensitivity and outputs give us confidence in the Canada-wide NPP spatial distribution patterns and the regional statistics presented in this paper.

Direction for further studies

Most current process models at the global and continent scales assume that the ecosystems are static, so that the effect of stand age on NPP is not addressed (Cramer *et al.*, 1999). Currently BEPS follows this assumption, except that the change of LAI with age is captured in the remote sensing data (Amiro *et al.*, 2000). As the boreal forest is disturbed by frequent wildfires and insect-induced mortality (Kurz & Apps, 1995), further investigation is needed to see whether LAI can capture most stand dynamics.

Although the nonlinear effects of meteorological variables on NPP within the daily time steps are much reduced using the integrated daily NPP model, errors may still exist because the general daily model cannot capture subdaily extreme events (Chen *et al.*, 1999). The accuracy of the NPP calculation can be improved further if the time step is reduced to minutes or hours. Such improvement could be realized by running the model in conjunction with a global circulation model.

Due to computational constraints, the topographical effects on soil water regimes have not explicitly been considered, and may introduce some errors in mountainous areas. Incorporating topographical data into the model in this way will reduce uncertainty in both carbon cycle and water cycle simulations, especially for mountainous area.

In this study, NPP values were compared with ground data from two forest regions. More work is required for NPP validation using a broad range of measurements, such as tower flux, tree ring and biomass measurements. The validation of such moderate resolution NPP maps would require the use of high resolution remote sensing images to locate the ground plots and to scale between pixels of various resolutions. However, the use of high-resolution images for this purpose would require the integration of BEPS with a watershed hydrological model to consider topographic effects on the soil water regimes of small pixels. This is our next intended step.

ACKNOWLEDGMENTS

We are grateful to Richard Fernandes for careful internal review and valuable comments and to Rasim Latifovic and Goran Pavlic for help in processing soil and other data. We are especially indebted to David Price at Canada Forest Service and Alain Royer at University of Sherbrooke for providing Forest Inventory and RESEF data, respectively. Data from Agriculture and Agri-Food Canada and the National Center for Atmospheric Research are appreciated. This research is supported by the Northern Biosphere Observation and Modelling Experiment (NBIOME).

REFERENCES

Aase, J.K., Millard, J.P. & Brown, B.S. (1986) Spectral radiance estimates of leaf area and leaf phytomass of small grains and native vegetation. *IEEE Transactions on Geoscience and Remote Sensing*, **24**, 685–692.

Amiro, B.D., Chen, J.M. & Liu, J. (2000) Net primary productivity following forest fire for Canadian ecoregions. *Canadian Journal of Forest Research*, **30**, 939–947.

Asrar, G., Fuchs, M., Kanemasu, E.T. & Hatfield, J.H. (1984) Estimating absorbed photosynthetic radiation and leaf area index from spectral reflectance in wheat. *Agronomy Journal*, **76**, 300–306.

Beaubien, J., Cihlar, J., Simard, G. & Latifovic, R. (1999) Land cover from multiple Thematic Mapper scenes using a new enhancement — classification methodology. *Journal of Geophysical Research*, **104**, 27 909–27 920.

Belward, A.S., ed. (1996) *The IGBP-DIS Global 1 Km Land-Cover Dataset (DISCOVER) — proposal and implementation plans*. IGBP-DIS Working Paper no. 13. IGBP-DIS, Toulouse, France.

Black, T.A., den Hartog, G., Neumann, H.H., Blanken, P.D., Yang, P.C., Russell, C., Nesic, Z., Lee, X., Chen, S.G., Staebler, R. & Novak, M.D. (1996) Annual cycle of water vapour and carbon dioxide fluxes in and above a boreal aspen forest. *Global Change Biology*, **2**, 101–111.

Bonan, G.B. (1993) Importance of leaf area index and forest type when estimating photosynthesis in boreal forests. *Remote Sensing of Environment*, **43**, 303–314.

Bonan, G.B. (1995) Land-atmosphere CO_2 exchange simulated by a land surface process model coupled to an atmospheric general circulation model. *Journal of Geophysical Research*, **100**, 2 817–2 812 831.

Bondeau, A., Kicklighter, D.W., Kaduk, J. & others (1999) Comparing global models of terrestrial net primary productivity (NPP): importance of vegetation structure on seasonal NPP estimates. *Global Change Biology*, **5**, 35–45.

Chen, W.J., Chen, J., Liu, J. & Cihlar, J. (2000) Approaches for reducing uncertainties in regional forest carbon balance. *Global Biogeochemical Cycle*, **14**, 827–838.

Chen, J.M., Chen, W., Liu, J. & Cihlar, J. (2000) Carbon budget of boreal forests estimated from the changes in disturbances, climate, nitrogen and CO_2: results for Canada in 1895–1996. *Global Biogeochemical Cycle*, **14**, 839–850.

Chen, J.M. & Cihlar, J. (1996) Retrieving leaf area index for boreal conifer forests using landsat TM images. *Remote Sensing of Environment*, **55**, 153–162.

Chen, J.M., Liu, J., Cihlar, J. & Goulden, M.L. (1999) Daily canopy photosynthesis model through temporal and spatial scaling for remote sensing applications. *Ecological Modelling*, **124**, 99–119.

Chen, J.M., Pavlic, G., Brown, L., Cihlar, J., Leblanc, S.G., White, P.H., Hall, R.G., Peddle, D., King, D.J., Trofymow, J.A., Swift, E., Van der Sanden, J. & Pellikka, P. (2002) Validation of Canada-wide leaf area index maps using ground measurements and high and moderate resolution satellite imagery. *Remote Sensing of Environment*, **80**, 165–184.

Cihlar, J. (1996) Identification of contaminated pixels in AVHRR composite images for studies of land biosphere. *Remote Sensing of Environment*, **56**, 149–163.

Cihlar, J., Beaubien, J., Latifovic, R. & Simard, G. (1999) *Land cover of Canada 1995*, version 1.1. Digital dataset documentation, Natural Resources Canada, Ottawa, Ontario. ftp.//ftp2.ccrs.nrcan.gc.ca/ftp/ad/EMS/landcover95/.

Cihlar, J., Chen, J. & Li, Z. (1997b) Seasonal AVHRR multichannel datasets and products for studies of surface–atmosphere interactions. *Journal of Geophysical Research*, **102**, 29 625–29 640.

Cihlar, J., Ly, H., Li, Z., Chen, J., Pokrant, H. & Huang, F. (1997a) Multitemporal, multichannel AVHRR datasets for land biosphere studies: artifacts and corrections. *Remote Sensing of Environment*, **60**, 35–57.

Cramer, W., Kicklighter, D.W., Bondeau, A., Morre, B. III, Churkina, G., Nemry, B., Ruimy, A., Schloss, A.L. & the participants of the Potsdam NPP Model Intercomparison (1999) Comparing global models of terrestrial net primary productivity (NPP): overview and key results. *Global Change Biology*, 5, 1–15.

De Jong, R., Shields, J.A. & Sly, W.K. (1984) Estimated soil water reserves applicable to a wheat-fallow rotation for generalized soil areas mapped in southern Saskatchewan. *Canadian Journal of Soil Science*, **64**, 667–680.

De Pury, D.G.G. & Farquhar, G.D. (1997) Simple scaling of photosynthesis from leaves to canopies without the errors of big-leaf models. *Plant, Cell and Environment*, **20**, 537–557.

Ecological Stratification Working Group (1995) *A national ecological framework for Canada*. Agriculture and Agri-Food Canada, Research Branch, Centre for Land and Biological Resources Research and Environment Canada, State of the Environment Directorate, Ecozone Analysis Branch, Ottawa/Hall, Canada.

Environment Canada (2000) *Climate trends and variation bulletin for Canada*. http://www.tor.ec.gc.ca/ccrm/bulletin/index.html.

Farquhar, G.D. & von Caemmerer, S. (1982) Modelling of photosynthetic response to environmental conditions. *Encyclopedia of plant physiology*, New Series, vol. 12b, *Physiological plant ecology II* (ed. by O.L. Lange, P.S. Nobel, C.B. Osmond and H. Ziegler), pp. 549–587. Spring-Verlag, Berlin, Germany.

Farquhar, G.D., von Caemmerer, S. & Berry, J.A. (1980) A biochemical model of photosynthetic CO_2 assimilation in leaves of C_3 species. *Planta*, **149**, 78–90.

Foley, J.A. (1994) Net primary productivity in the terrestrial biosphere: the application of a global model. *Journal of Geophysical Research*, **99**, 20 773–20 783.

Foley, J.A., Prentice, I.C., Ramankutty, N., Levis, S., Pollard, D., Sitch, S. & Haxeltine, A. (1996) An integrated biosphere model of land surface processes, terrestrial carbon balance and vegetation dynamics. *Global Biogeochemical Cycles*, **10**, 603–628.

Frolking, S. (1997) Sensitivity of spruce/moss boreal forest net ecosystem productivity to seasonal anomalies in weather. *Journal of Geophysical Research*, **102**, 2 229 053–2 229 064.

Gagnon, G., Gravel, C., Ouimet, R., Dignard, N., Paquin, R. & Jacques, G. (1994) *Le Réseau de surveillance des écosystèmes forestiers (RESEF). II — Description des places d'étude et données de base*. Mémoire de Recherche Forestière no. 116. Ministères des Ressources Naturelles, Québec.

Goulden, M.L., Daube, B.C., Fan, S.-M., Sutton, D.J., Bazzaz, A., Munger, J.W. & Wofsy, S.C. (1997) Physiological responses of a black spruce forest to weather. *Journal of Geophysical Research*, **102**, 28 987–28 996.

Haxeltine, A. & Prentice, I.C. (1996) BIOME3: an equilibrium terrestrial biosphere model based on ecophysiological constraints, resource availability, and competition among plant functional types. *Global Biogeochemical Cycles*, **10**, 693–709.

Hunt, E.R., Piper. S.C., Nemani, R., Keeling, C.D., Otto, R.D. & Running, S.W. (1996) Global net carbon exchange and intra-annual atmospheric CO_2 concentrations predicted by an ecosystem simulation model and three-dimensional atmospheric transport model. *Global Biogeochemical Cycles*, **10**, 431–456.

Kimball, J.S., Thornton, P.E., White, M.A. & Running, S.W. (1997) Simulating forest productivity and surface-atmosphere carbon exchange in the BOREAS study region. *Tree Physiology*, **17**, 589–599.

Kurz, W.A. & Apps, M.J. (1995) An analysis of future C budgets of Canadian boreal forests. *Water, Air, and Soil*, **82**, 321–331.

Kurz, W.A., Beukema, S.J. & Apps, M.J. (1996) Estimation of root biomass and dynamics for the carbon budget model of the Canadian forest sector. *Canadian Journal for Forest Research*, **26**, 1973–1979.

Lavigne, M.B. & Ryan, M.G. (1997) Growth and maintenance respiration rates of aspen, black spruce and jack pine stems at northern and southern BOREAS sites, *Tree Physiology*, **17**, 543–551.

Li, Y., Demetriades-Shah, T.H., Kanemasu, E.T., Shultis, J.K. & Kirkham, M.B. (1993) Use of second derivatives of canopy reflectance for monitoring prairie vegetation over different soil backgrounds. *Remote Sensing of Environment*, **44**, 81–87.

Liu, J., Chen, J.M., Cihlar, J. & Chen, W. (1999) Net primary productivity distribution in the BOREAS region from a process model using satellite and surface data. *Journal of Geophysical Research*, **104**, 27 735–27 754.

Liu, J., Chen, J.M., Cihlar, J. & Park, W.M. (1997) A process-based boreal ecosystem productivity simulator using remote sensing inputs. *Remote Sensing of Environment*, **62**, 158–175.

Lowe, J.J., Power, K. & Gray, S.L. (1996) *Canada's forest inventory 1991: the 1994 version*. Information Report BC-X-364E. Pacific Forestry Centre, Canadian Forest Service, Natural Resources Canada, Victoria, BC, Canada.

Melillo, J.M. & VEMAP members (1995) Vegetation/ecosystem modeling and analysis project: Comparing biogeography and biogeochemistry models in a continental-scale study of terrestrial ecosystem responses to climate changes and CO_2 doubling. *Global Biogeochemical Cycles*, **9**, 407–437.

Middleton, E.M., Sullivan, J.H., Bovard, B.D., Deluca, A.J., Chan, S.S. & Cannon, T.A. (1997) Seasonal variability in foliar characteristics and physiology for boreal forest species at the five Saskatchewan tower sites during the 1994 Boreal Ecosystem-Atmospheric Study. *Journal of Geophysical Research*, **102**, 28 831–28 844, 770.

Norman, J.M. (1993) Scaling processed between leaf and canopy levels. *Scaling physiological processes: leaf to globe* (ed. by J.R. Ehleringer & C.B. Field), pp. 41–76. Academic Press, San Diego.

Olson, J.S. (1994*) Global ecosystem framework-definitions*. USGS EROS Data Centre Internal Report. USGS EROS Data Centre, Sioux Falls, South Dakota.

Peng, C. & Apps, M. (1999) Modelling the response of net primary productivity (NPP) of boreal forest ecosystems to changes in climate and fire disturbance regimes, *Ecological Modelling*, **122**, 175–193.

Penner, M., Power, K., Muhairwe, C., Tellier, R. & Wang, Y. (1997) *Canada's forest biomass resources: deriving estimates from Canada's forest inventory*. Information Report BC-X-370. Pacific Forestry Centre, Canadian Forest Service, Natural Resources Canada, Victoria, BC, Canada.

Pietroniro, A. & Soulis, E.D. (1999) Assessment of global land-cover data for atmospheric and hydrologic model applications in the Mackenzie basin, Canada. *Proccedings of the 5th Scientific Workshop for the Mackenzie GEWEX Study, Edmonton, Alberta*, Canada, 21–23. November, 1999.

Pokrant, H. (1991) *Land-cover map of Canada derived from AVHRR images*. Manitoba Remote Sensing Centre, Winnipeg, Manitoba, Canada.

Potter, C.S., Wang, S., Nikolov, N.T., McGuire, A.D., Liu, J., King, A.W., Kimball, J.S., Grant, R.F., Frolking, S.E., Clein, J.S., Chen, J.M. & Amthor, J.S. (2001) Comparison of boreal ecosystem model sensitivity to variability in climate and forest site parameters. *Journal of Geophysical Research*, **106**, 33 671–33 688.

Potter, C.S., Randerson, J.T., Field, C.B., Matson, P.A., Vitousek, P.M., Mooney, H.A. & Klooster, S.A. (1993) Terrestrial ecosystem production: a process model based on global satellite and surface data. *Global Biogeochemical Cycles*, **7**, 811–841.

Running, S.W. & Coughlan, J.C. (1988) A general model of forest ecosystem processes for regional applications I. Hydrological balance, canopy gas exchange and primary production processes. *Ecological Modelling*, **42**, 125–154.

Running, S.W. & Hunt, E.R. (1993) Generalization of a forest ecosystem process model for other biomes, BIOME-BGC, and an application for global scale models. *Scaling physiological processes: leaf to globe* (ed. by J.R. Ehleringer & C.B. Field), pp. 141–158. Academic Press, San Diego.

Running, S.W., Nemani, R.R., Peterson, D.L., Band, L.E., Potts, D.F., Pierce, L.L. & Spanner, M.A. (1989) Mapping regional forest evapotranspiration and photosynthesis by coupling satellite data with ecosystem simulation. *Ecology*, **70**, 1090–1101.

Ryan, M., Lavigne, M.B. & Gower, S.T. (1997) Annual carbon cost of autotrophic respiration in boreal forest ecosystems in relation to species and climate. *Journal of Geophysical Research*, **102**, 28 871–28 883.

Sellers, P.J., Los, S.O., Tucker, C.J., Justice, C.O., Dazlich, D.A., Collatz, G.J. & Randall, D.A. (1996) A revised land surface parameterization (SiB2) for atmospheric GCMs. Part II: the generation of global fields of terrestrial biophysical parameters from satellite data. *Journal of Climate*, **9**, 706–737.

Sellers, P. & others (1995) The boreal ecosystem-atmosphere study (BOREAS): an overview and early results from the 1994 field year. *Bulletin of the American Meteorological Society*, **76**, 1549–1577.

Shields, J.A., Tarnocai, C., Valentine, K.W.G. & MacDonald, K.B. (1991) *Soil landscapes of Canada, procedures manual and user's handbook*. Agriculture Canada Publication 1868/E. Agriculture Canada, Ottawa, Ontario.

Siltanen, R.M. & Price, D.T. (2001) *A 10 km rasterized data base of Canada's forest biomass derived from Canada's forest inventory, 1991*. Northern Forestry Centre, Canada Forest Service.

Statistics Canada (1995) *Grain trade of Canada*, Catalogue 22–201. Statistics Canada, Ottawa, Canada.

Warnant, P., Francois, L., Strivay, D. & Gérard, J.-C. (1994) CARAIB: a global model of terrestrial biological productivity. *Global Biogeochemical Cycles*, **8**, 255–270.

Wiegand, C.L., Maas, S.J., Aase, J.K., Hatfield, J.L., Pinter, P.J., Jr Jackson, R.D., Kanemasu, E.T. & Lapitan, R.L. (1992) Multisite analyses of spectral-biophysical data for wheat. *Remote Sensing of Environment*, **42**, 1–21.

Woodward, F.I., Smith, T.M. & Emanuel, W.R. (1995) A global land primary productivity and phytogeography model. *Global Biogrochemical Cycles*, **9**, 471–490.

Wullschleger, S.D. (1993) Biochemical limitations to carbon assimilation in C_3 plants — a retrospective analysis of the A/C_i curves from 109 species. *Journal of Experimental Botany*, **44**, 907–920.

BIOSKETCHES

Jane Liu is an environmental scientist at the Canada Centre for Remote Sensing (CCRS). She is interested in studies on the interaction between atmosphere and biosphere using techniques in numerical simulation, remote sensing, and GIS.

Dr J. Chen is a professor in the Department of Geography at the University of Toronto. His main research areas include retrieving biophysical parameters from remotely sensed data, radiation modelling, and biogeochemical cycle modelling.

Dr Cihlar is a senior research scientist and Head of the Environmental Monitoring Section at CCRS. His primary research interests are in the use of satellite observations to understand the dynamics of terrestrial ecosystems.

Dr W. Chen is a research scientist at CCRS. His main research interest includes national-scale carbon and hydrological cycle studies using remote sensing and ground data.

APPENDIX 1

Key equations in the Boreal Ecosystem Productivity Simulator (BEPS)

Annual NPP (in g C m^{-2} $year^{-1}$) is accumulated from the difference between gross primary productivity (*GPP*) and autorespiration (R_a) on each day, i.e.

$$NPP = \sum_{i=1}^{365} (GPP - R_a) \quad \text{(A1)}$$

Daily gross primary productivity

The Farquhar model (Farquhar *et al.*, 1980) is adopted and modified for *GPP* calculation. Because the Farquhar model was initially developed for individual leaves at an instant of time, care must be taken in using it for a plant canopy for a time period, such as a day. BEPS uses the sunlit and shaded leaf separation approach strategy (Norman, 1993; Foley *et al.*, 1996; De Pury & Farquhar, 1997) after some modifications (Chen *et al.*, 1999). This stratification strategy is preferred over the multi-layering strategy (Bonan, 1995) for its ability to capture the major radiation variation within the canopy at a given time, enabling effective temporal integration (Chen *et al.*, 1999). With the separation of sunlit and shaded leaf groups, the daily canopy total *GPP* can be calculated as (Norman, 1993):

$$GPP = (A_{sun}\, LAI_{sun} + A_{shade}\, LAI_{shade})\, Day\_Length\, Factor_{GPP} \quad \text{(A2)}$$

where the subscripts 'sun' and 'shade' denote the sunlit and shaded components of daily mean photosynthesis rate (*A*) and leaf area index (*LAI*). $Factor_{GPP}$ converts *GPP* unit into g C m^{-2} day^{-1}.

Mean photosynthesis rate *A* can be calculated with eqn A3 for sunlit and shaded leaf separately, while procedures to obtain LAI_{sun} and LAI_{shade} are available in Liu *et al.* (1999). The formula for *A* is derived after the analytical integration of the Farquhar model over a day to consider the nonlinear effects of meteorological variables on photosynthesis due to their diurnal variability, through several steps of mathematical development (Chen *et al.*, 1999; Liu *et al.*, 1999):

$$A = \frac{1.27}{2(g_n - g_{\min})}\left(\frac{a^{1/2}}{2}(g_n^2 - g_{\min}^2) + c^{1/2}(g_n - g_{\min}) - \frac{2ag_n + b}{4a}d + \frac{2ag_{\min} + b}{4a}e + \frac{b^2 - 4ac}{8a^{3/2}}\ln\frac{2ag_n + b + 2a^{1/2}d}{2ag_{\min} + b + 2a^{1/2}e}\right) \quad \text{(A3)}$$

where *A* is the minimum of Rubisco-limited photosynthesis rate A_c and light limited photosynthesis rate A_j in μmol m^{-2} s^{-1}. For A_c, $a = (K + C_a)^2$, $b = 2(2\Gamma + K - C_a)V_m + 2(C_a + K)R_d$, and $c = (V_m - R_d)^2$. For A_j, $a = (2.3\Gamma + C_a)^2$, $b = 0.4(4.3\Gamma - C_a)J + 2(C_a + 2.3\Gamma)R_d$, and $c = (0.2\,J - R_d)^2$. For both, $d = (ag_n^2 + bg_n + c)^{1/2}$ and $e = (ag^2{}_{\min} + bg_{\min} + c)^{1/2}$. Note *a*, *b*, *c* and *d* are calculated with the leaf biochemical parameters in the original Farquhar model with no additional parameters. C_a is the CO_2 concentration in the atmosphere, set as a constant of 36 Pa at present. R_d is daytime leaf dark respiration in μmol m^{-2} s^{-1}. Γ is the CO_2 compensation point without dark respiration; *K* is a function of enzyme kinetics. The dimension for Γ, *K* can be in Pa. Both Γ and *K* are temperature-dependent parameters. $g_{\min}$ is the minimum, stomatal conductance, assuming to be zero in this study. g_n is the stomatal conductance at noon in μmol m^{-2} s^{-1}, which is controlled by radiation, air temperature, air humidity and soil water condition of the day (Liu *et al.*, 1999). V_m is the maximum carboxylation rate in μmol m^{-2} s^{-1}, and *J* is the electron transport rate in μmol m^{-2} s^{-1}. Daily mean of V_m and *J* are estimated from daily radiation, temperature and other parameters (Farquhar & Caemmerer, 1982; Wullschleger, 1993; Bonan, 1995):

$$V_m = V_{m25}\, 2.4^{(T-25)/10}\, (N/N_m)\left[1 + \exp\left(\frac{-220\,000 + 710(T + 273)}{R_{gas}(T + 273)}\right)\right] \quad \text{(A4)}$$

$$J = I(29.1 + 1.64V_m)/(I + 2.1(29.1 + 1.64V_m)) \quad \text{(A5)}$$

where V_{m25} is the maximum carboxylation rate at 25 °C in μmol m^{-2} s^{-1}. N/N_m is ratio of foliage nitrogen concentration to maximum foliage nitrogen concentration. R_{gas} is molar gas constant (= 8.3143) m^3 mol^{-1} K^{-1}. *T* is air temperature in °C. *I* is photosynthetically active flux density in μmol m^{-2} s^{-1}.

Daily autorespiration

Daily autotrophic respiration (R_a) (in g C m^{-2} day^{-1}) is broken into maintenance respiration (R_m) and growth respiration (R_g) (Running & Coughlan, 1988):

$$R_a = R_m + R_g \quad \text{(A6)}$$

For forest with biomass data, maintenance respiration is the sum of the maintenance respiration of each plant component, i.e.:

$$R_{m,i} = M_i r_{m,i} Q_{10,i}^{(T-T_b)/10} \quad \text{(A7)}$$

where i defines a plant component, such as leaf, stem and root. M_i is biomass (sapwood for stems, estimated from stem biomass) of a plant component i; $r_{m,i}$ maintenance respiration coefficient for component i; $Q_{10,i}$ the temperature sensitivity factor for component i, and T_b the base temperature. $Q_{10,i}$ and T_b are the same as in Ryan *et al*. (1997) and Lavigne & Ryan (1997), respectively.

For all other land cover types without biomass data, maintenance respiration is estimated using LAI (Bonan, 1995):

$$R_m = LR_{f25}(1 + p)2.0^{(T-25)/10} Factor_{rm} \quad \text{(A8)}$$

where L is the total leaf area index. R_{f25} is foliage respiration at 25 °C and p accounts for nonfoliage contribution to maintenance respiration, both available from Bonan (1995). $Factor_{rm}$ here converts R_m from μmol m^{-1} s^{-2} into g C m^{-2} day^{-1}.

Finally, growth respiration is treated to be proportional to daily gross productivity for all land cover types:

$$R_g = r_g GPP \quad \text{(A9)}$$

where r_g is a growth respiration coefficient, being 0.25 (Bonan, 1995).